



## Numerical Evaluation of Slope Stability for Construction and Seismic Loads: Case Study

Z. Alsharifi<sup>a</sup>, M. Shakir Mahmood<sup>\*a</sup>, A. Akhtarpour<sup>b</sup>

<sup>a</sup> Civil Engineering Department, University of Kufa, Al-Najaf, Iraq

<sup>b</sup> Civil Engineering Department, Ferdowsi University of Mashhad, Mashhad, Iran

### PAPER INFO

#### Paper history:

Received 28 March 2021

Received in revised form 17 May 2021

Accepted 18 May 2021

#### Keywords:

Slope Stability

Finite Element Method

Strip Footing

Earthquake

### ABSTRACT

Al-Najaf, one of Iraq's most important cities, is expected to grow in the coming years. Many buildings located on the slopes of Al-Najaf, which is near the shrine of Imam Ali, possess important economic and tourism values. This paper examines the stability of the city's slope under a variety of conditions, including slope geometry, neighbor structure loading, and earthquake magnitude. A computer-aided 2D Finite Element Method is adopted in the analysis. A set of soil classification and identification tests were carried out in addition to the available required soil parameters in the constitutive modeling. The Mohr-Coulomb model is applied to define the failure state that began in the slope. The results show that the slope is stable due to its weight and geometry, with a minimum factor of safety of 2.6. While under footing loading, this factor of safety decreases to less than 1.8. The most hazardous condition is when the slope has been subjected to seismic loading and the factor of safety is less than unity, for all investigated cases and characteristics, where the slopes would collapse.

doi: 10.5829/ije.2021.34.07a.05

### NOMENCLATURE

A	Footing area (m <sup>2</sup> )	PI	Plastic index
B	Strip footing width (m)	q <sub>u</sub>	Bearing capacity(kPa)
C <sub>c</sub>	Coefficient of curvature	X	Distance from slope edge to the footing (m)
C <sub>u</sub>	Coefficient of uniformity	<b>Greek Symbols</b>	
C	Cohesion (kPa)	σ	Normal stress(kPa)
D	Damping Ratio	σ' <sub>m</sub>	Mean stress(kPa)
E	Yong's modulus	θ	Slope angle (degree)
FS	Factor of safety	τ <sub>f</sub>	Failure shear stress (kPa)
G	Shear modulus(kPa)	φ	Internal friction Angle (degree)
G <sub>max</sub>	Maximum shear modulus(kPa)	γ <sub>dry</sub>	Dry soil density (g/cm <sup>3</sup> )
G <sub>s</sub>	Specific gravity	γ <sub>c</sub>	Cyclic shear strain
H	Slope height (m)	ω	Natural Moistness content
k	Permeability (m/s.)	ν	Poisson's ratio
P	Applied load (kN)	ε	Strain
P <sub>a</sub>	Atmospheric pressure(kPa)		

## 1. INTRODUCTION

Flatland shortage and rapid development in hilly terrain with appealing sights are impacting construction on

hillsides, and so are many urban excavations in the vicinity of existing structures [1].

Rainfall, earthquakes, erosion, geological characteristics, and construction events are the factors that can cause slope failure. The slope stability analyses are demonstrated on hypotheses, where the

\* Corresponding Author Email: [mohammedsh.alshakarchi@uokufa.edu.iq](mailto:mohammedsh.alshakarchi@uokufa.edu.iq) (M. Shakir Mahmood)

configuration of the slope depends on practice and reliable inspection, (faults, stratification, etc.) [2].

The forms of a slope failure can be classified as, fall, topple slide, spread, and flow [3].

The limit equilibrium methods are suitable for practical purposes where the equilibrium equations are less than the unknowns in slope stability problems, and with assumptions, the problem can be reformed from indeterminate to determinate [4].

The stabilization of footings adjacent to the slope and the slope is obligatory since both bearing capacity and slope stability need to be revealed [5, 6]. Plentiful standards and codes primarily focus on the footings' design in flatlands, giving unsuitable guidelines for the constructions near the slope [5].

Enormous earthquakes are significant in slope collapse [7]. For seismic loading with a decreased soil bearing capacity and an increase in deformation, the security of structures should be assured in recently constructed [8, 9]. The input parameters include characteristics, the earthquake magnitude, frequency, intensity of ground motions, and period of a shake [10].

Iraq is positioned in a seismically active zone and, as a result, is an instability region that has undergone many powerful earthquakes in recent decades. Extreme events have taken numerous lives, damaged several towns, and caused extensive financial harm in this era. The last enormous seismic event was struck at Iran- Iraq frontier in November 2017 [11].

The challenge of a loaded slope with footing has been widely analyzed in a normal loading state, static load. Yet, the dynamic analysis of a loaded slope exposed to seismic force was not thoroughly explored. However, limit equilibrium analysis was employed to inspect the stability of dynamically loaded slope [12].

The soil's shear strength can be enhanced by the long term soaking method [13]. The risk of collapse in all soil groups rises due to a drop in soil matric suction [14-16].

The Mohr-Coulomb model (elastic-perfectly plastic model) is the simplest method for representing soil failure in constitutive models, giving conservative values to all inspected parameters of the footing and dam soils when compared to the Modified Cam-Clay modeling (elastoplastic model) [17-19].

For several years, slope stability analysis that used the finite element approach has been commonly recognized in the literature. The major finite element slope stability approaches used today are the enhanced limit strength method and the strength reduction method. Similarities of the finite element and limit equilibrium approach analyses of slope stability demonstrate the benefits and drawbacks of these approaches for convenient technical challenges [20].

Even though many modern numerical approaches, including the finite element method, have been introduced over the last three decades; the traditional limit equilibrium procedure has remained the most effective in slope stability analysis. Moreover, because of the finite element method's numerous benefits over the limit equilibrium method, However, due to the numerous benefits of the finite element method above the limit equilibrium method, the finite element method now has an increase in applications for stability analysis [21].

The recent paper focuses on the stability analysis of Al-Najaf city's slope under different geometry and loading conditions. The assessment of the slope is important due to the attraction and it is the first numerical model be made for the slopes of Al-Najaf city for the effect of adjacent buildings, earthquakes and for its specific soil characteristics.

## 2. RESEARCH METHODOLOGY

**2.1. Materials** The study area is located within the slope that lay beside Al-Najaf old city and near to the shrine of Imam Ali in south-western of Iraq, as shown in Plate 1. between the longitude lines of  $43^{\circ} 00'$  and  $44^{\circ} 30'$  and latitudes of  $30^{\circ} 45'$  and  $32^{\circ} 15'$ . This location has recently developed, and more development is expected as a result of the city's religious attraction. Construction is one of the development aspects, and there is a need to investigate the city's slope instability caused by the extra loading from neighboring construction, earthquakes and rainfall.

The samples were collected from three different sites along the slope with symbols of S1, S2, and S3, as shown in Plate 2.

A set of tests were conducted on the soil samples from the slope site according to ASTM procedures. Figure 1 illustrates the grain size distribution of the different soil samples and reveals that all soil samples are similar in gradation. For this reason, a standard Proctor test is performed for S2, as shown in Figure 2. Table 1 summarizes the results of soil identification and classification tests. The soil samples are classified according to the Unified Soil Classification System (USCS) as 'SP'. These data are important to select the soil density, angle of internal friction, permeability coefficient, and Yong's modulus.

Many other soil properties are required for the selected constitutive model. Many site investigations and papers are published concerning the soil mechanical properties which are computed through experimental work. Table 2 illustrates the selected input soil properties.

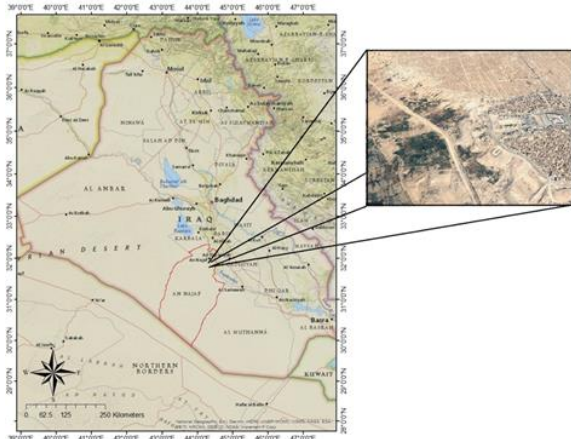


Plate 1. The site of research area

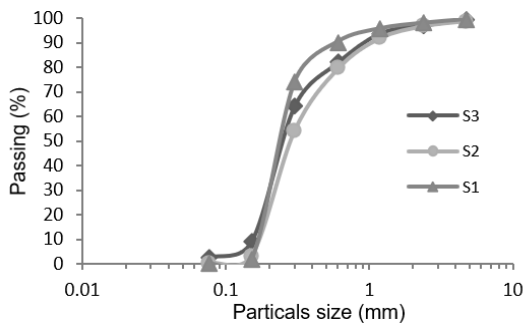


Figure 1. Grain size distribution of the soil samples

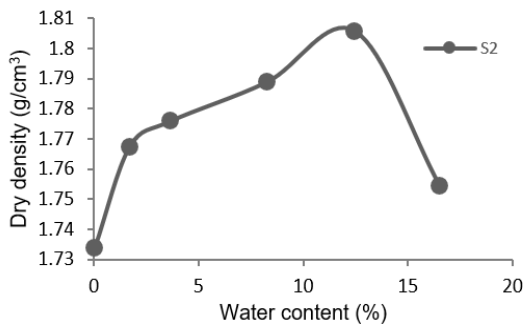


Figure 2. Standard Proctor test results

**2. 2. Slope Geometry** Using the software titled "Google Earth", the height and angle of the slope are determined. Plate 2 shows the sections of the slope geometry measurements. The height of the slope is ranged between 16 m and 24 m where the slope angle is ranged between 4° and 9° as shown in Table 3.

The slope safety is examined in this paper for the various geometry boundaries where the slope heights (H) are 15, 20 and 30 m and the slope angles (θ) are 5, 7, 10 and 15 degrees.

**2. 3. Loading** A static load represented by building with strip footing is covered in this study

which had a constant applied stress equal to 85 kPa. The study investigates a different footing width (B) and distance from the slope edge (X), as shown in Figure 3.

To investigate the effect of the most dangerous earthquake case that occurred in Iraq, Halabjah earthquake, 2017 returning quake on Kirkuk, North-South direction (with magnitude of 4.9) data (acceleration time history) was adopted from literature [22].

TABLE 1. The results of soil identification tests

Soil identification	S-1	S-2	S-3
Sand, %	99.09	98.66	96.73
Fine, %	0.34	0.33	2.65
D <sub>10</sub> , mm	0.167	0.170	0.153
D <sub>30</sub> , mm	0.208	0.229	0.207
D <sub>60</sub> , mm	0.271	0.368	0.289
Coefficient of uniformity (Cu)	1.623	2.167	1.891
Coefficient of curvature (Cc)	0.961	0.836	0.973
Soil Classification (USCS)	SP	SP	SP
Natural Moistness content (w), %	3.14	3.51	5.05
Maximum dry density(γ <sub>dry</sub> ), g/cm <sup>3</sup>	-	18.06	-
Optimum moisture content, %	-	12.47	-
Specific gravity (Gs)	2.623	2.622	2.633
Gypsum content, %	-	1.23	-

TABLE 2. Additional necessary soil properties

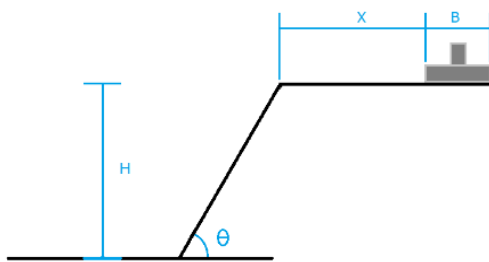
Soil properties	Min.	Max.	Avg.
Angle of internal friction (Φ), deg. [23]	30	35	33
Cohesion (C), kPa [23]	0	0	0
Bearing capacity, kPa [23]	70	100	85
Yong's modulus (E), kPa [24]		20125	
Poisson's ratio (ν) [24]		0.35	



Plate 2. The investigation of slope geometry

**TABLE 3.** The geometry of the city's slopes

Section	Slope height (H), m	Slope angle ( $\theta$ ), deg.
1	24	6.36
2	21	4.92
3	16	4.16
4	29	9.02
5	19	7.61
6	24	7.10
7	16	6.80
8	21	7.72

**Figure 3.** Sketch of slope's investigated parameters

**2. 4. Constitutive Model** The Finite Element Method (FEM) is performed for numerical analysis. The analysis depended on the principle of limit equilibrium, which combines a finite element method that is advanced, especially for the stability and deformation of slopes and embankment structures [25].

The case study in this study were modeled in two-dimensional finite element of quads and triangle mesh with global elements size equal to 8 m and a 0.24m mesh size for the ground surface of the model. The integration order were 4 nodes for quadrilateral elements and 3 nodes for triangular elements in addition to secondary nodes on the boundary.

The fundamentals of the soil modeling program, using the gathered parameters of the study area (Tables 1 and 2), are explained as the following: The Mohr-Coulomb formula, Equation (1), is applied to define the failure state that began on the slope [26]:

$$\tau_f = C + \sigma \tan \phi \quad (1)$$

The soil has an elastic, perfectly-plastic with regular stress-strain relationships. Stresses are directly proportional to strains until the yield point is reached. Past the yield point, the stress strain curve is faultlessly horizontal (behaves linearly), with two parameters from Hooke's law: Young's modulus ( $E=20125$  kPa) and Poisson's ratio ( $\nu=0.35$ ). As well as two parameters which describe the failure conditions: the internal friction angle ( $\phi=35^\circ$ ) and cohesion ( $C=0$ ) [27].

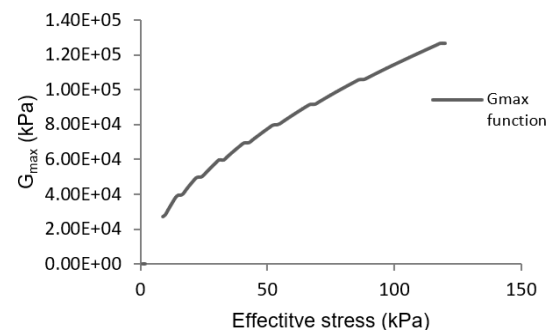
The soil will be modeled using an equivalent linear method during the dynamic analysis. Equation (2) states the linear relationship between stress and strain using the proportionality factor of Young's modulus. Yet, the variation is that the shear modulus is changed in response to strains. With the defined soil stiffness, identifying the maximum shear strains for each Gauss numerical integration point in each element. The shear modulus is then adjusted in accordance with a predetermined G reduction function, and the step was repeated. This iterative process is repeated until the required G adjustments are made according to shear strain. G is a constant when stepping via the earthquake record, which is an important behavior to understand. G can be changed by each pass via the record, but it always stays constant during a single pass [28].

$$\sigma = E \varepsilon \quad (2)$$

In this study, Equation (3) was provided to determinate shear modulus (G) during the analysis stages by inbuilt function. For medium dense sand (as it appear from sieve analysis data and the value of internal friction angle  $\phi$ ),  $K=50$ , where K is a parameter based on soil type found by Seed and Idriss [29], plastic index (PI)=0 and  $\gamma_{dry}=18$  KN/m<sup>3</sup> giving the  $G_{max}$  function (Figure 4) for the slopes' soil according to Equation (3).

$$G_{max} = 22K\sqrt{P_a\sigma'_m} \quad (3)$$

A dynamically stressed soil will be "softer" in contrast to cyclic shear stress. This softness is explained as a ratio of  $G_{max}$  in the Equivalent Linear modeling. This is known as G-reduction function. For the calculation of new G values in each iteration, the determined shear strain along with the function and  $G_{max}$  is used. Equations (4), (5) and (6) express a formula for calculating the  $G/G_{max}$  ratio [28] using plastic index (PI)=0 and  $\gamma_{dry}=18$  kN/m<sup>3</sup> gives the G-reduction function (Figure 5) for the slopes' soil according to Equation (4).

**Figure 4.** Max. shear modulus ( $G_{max}$ ) function of the studied soil according to Equation (3)

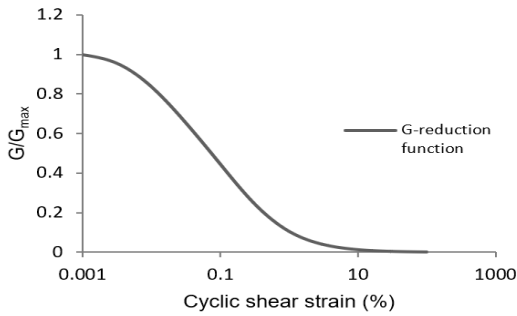


**Figure 5.** G-reduction function of the studied soil according to Equation (4)

$$\frac{G}{G_{max}} = K(\gamma, PI) (\sigma'_m)^{m(\gamma, PI) - m_0} \quad (4)$$

$$K(\gamma, PI) = 0.5 \left[ 1 + \tanh\left(\ln\left(\frac{0.000102 + n(PI)}{\gamma}\right)^{0.492}\right) \right] \quad (5)$$

$$m(\gamma, PI) - m_0 = 0.272 \left[ 1 - \tanh\left(\ln\left(\frac{0.000556}{\gamma}\right)^{1.1}\right) \right] \exp(-0.0145 PI^{1.2}) \quad (6)$$

The damping ratio was also generated from a inbuilt function (Equation (7)) was developed by Kramer [30] using plastic index (PI)=0 and  $\gamma_{dry} = 18 \text{ kN/m}^3$  gives the Damping function (Figure 6) for the slopes' soil according to Equation (7).

$$D = 0.333 \frac{1 + e^{-0.0145 PI^{1.2}}}{2} \left( 0.586 \left(\frac{G}{G_{max}}\right)^z - 1.547 \frac{G}{G_{max}} + 1 \right) \quad (7)$$

The validation of the numerical modeling of this research was not done using models for the study area soil and slope properties as this research is an original study, a verification is made by comparison of the results with published limit equilibrium calculations. Three modeles were exploit:

1. A hand calculation based on limit equilibrium methods published by GEO-SLOPE International Ltd. (homogeneous soil, 2:1 slope H=10 m,  $\gamma = 20 \text{ kN/m}^3$ ,  $C'=5 \text{ kPa}$  and  $\phi' = 30^\circ$ ).

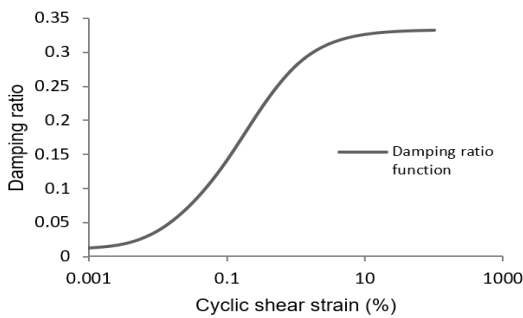


**Figure 6.** Damping ratio function of the studied soil according to Equation (7)

2. Verification problem#1in SLIDE verification manual (homogeneous soil, 2:1 slope H=10 m,  $\gamma = 20 \text{ kN/m}^3$ ,  $C'=3 \text{ kPa}$  and  $\phi' = 19.6^\circ$ ).
3. Verification problem#14 in SLIDE verification manual (homogeneous soil, 3:2 slope H=20 m,  $\gamma = 18.82 \text{ kN/m}^3$ ,  $C'=41.65 \text{ kPa}$  and  $\phi' = 15^\circ$ ).

The results gave a good agreement between the analysis for the inspected models ( $1 \geq R^2 > 0.97$ ).

### 3. RESULTS AND DISCUSSION

#### 3. 1. Effect of Slope Geometry

Figure 7 illustrates an example of slope slip surface and factor of safety in the case of the highest values of slope height (H) and angle ( $\theta$ ). Figure 8 provides the factor of safety values for various investigated slope heights and angles. Noticeably, there is a strong impact from slope angle on the safety where the effect of the slope height is marginal within the investigated ranges (critical values of the city's slope). These results are matched with literature [31], and may be attributed to the significant effect of the slope angle on the force component that is parallel to the slip surface where the failure occurs when the shear force is larger than the shear strength of the soil [32].

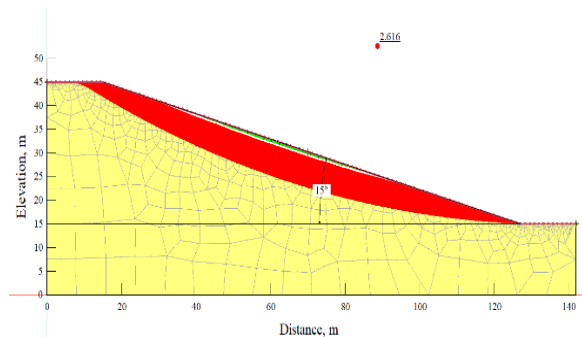


**Figure 7.** Slope Dermtation with Slope height (H) of 30m and Slope angle ( $\theta$ ) of 15degree

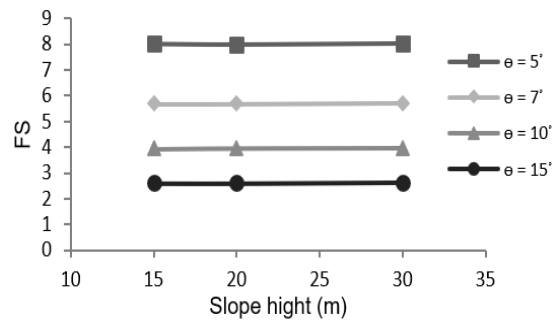


**Figure 8.** The effect of slope geometry on factor of safety

The minimum value of factor of safety is about 2.6, indicating that the slope in Al-Najaf is safe within the investigated geometry.

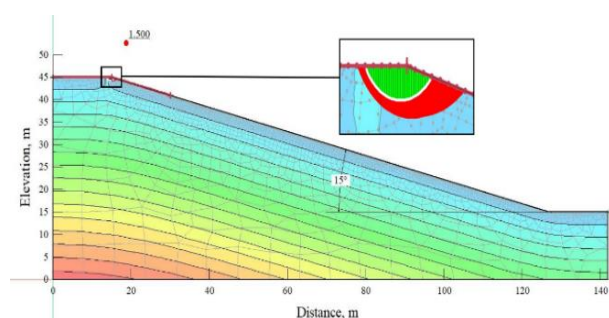
**3. 2. Effect of Neighbor Construction** The effect of strip footing width ( $B$ ) and its distance from the slope edge ( $X$ ) are investigated. For all cases with neighbor footing, a fixed applied stress of 85 kPa is given. Figure 9, as an example, proves that the failure in the slope of the city due to the specific footing is locally, i.e., the slope is safe and the failure is due to pressure limit of the footing and it matched with findings of failure modes by Mofidi et. al. [5].

Generally, there is a decrease in the factor of safety (FS) due to the application of the footing with respect to the initial condition (before construction). Figure 10 illustrates the effect of footing width on FS of the slope. There is a slight relationship between footing width and FS where this behavior is reflected in the increase of bearing capacity ( $q_u$ ) of the footing with the increase of its width. The rise in  $q_u$  may be credited to the bigger interaction area between footing and subsoil [33].

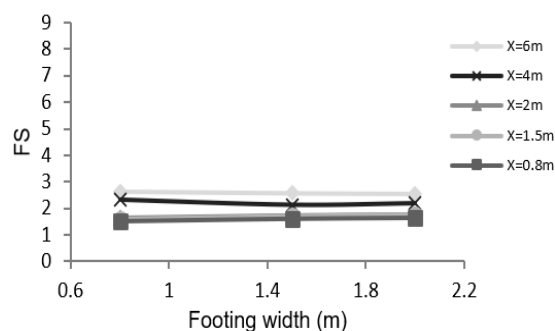
Obviously, there is a local failure (due to footing pressure) where the footing is closer to the slope ( $X=1.8-2\text{m}$ ). The maximum FS decreases with the existence of building footing to less than 1.8, yet, the distance between footing and slope crest effects FS with direct proportion.

Figure 11 verifies the effect of footing distance ratio ( $X/B$ ) on the factor of safety of the slope. The results indicate that the FS increases with increasing  $X/B$ . When the footing is moved away from the slope crest ( $X/B=4$ ), there is a clear increase in FS (about 50%). Nevertheless, the rate of increase in FS decreases with increasing distance beyond  $X/B=4$  where the failure due to bearing capacity is dominated.

The influence of slope is lessened when the footing is sited at an edge distance above four times the width of the footing. This increase in FS with respect to slope crest distance could be return to ground passive resistance from the slope edge [33].



**Figure 9.** Slope failure with Footing of 0.8m in Width at a distance ( $X$ ) of 0.8m for Slope of  $H=30\text{m}$  and  $\theta=15^\circ$



**Figure 10.** The effect of footing width on slope factor of safety for slope ( $H=30\text{m}$  and  $\theta=15^\circ$ )

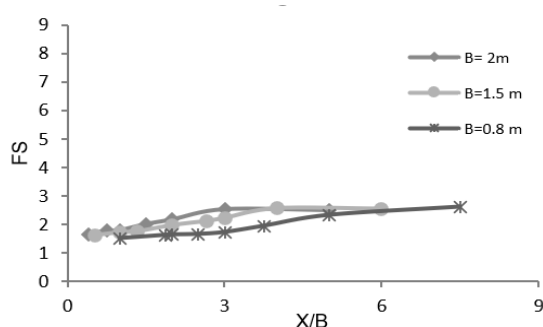


**Figure 11.** The relationship between factor of safety and  $X/B$  for slope ( $H=30\text{m}$  and  $\theta=15^\circ$ )

**3. 3. Effect of Seismic Load** To investigate the effect of the earthquake on the stability of the slope in Al-Najaf city, an earthquake of 4.9 magnitude is applied to the 30m height ( $H$ ) and different inclination slope ( $\theta=7^\circ, 10^\circ$  and  $15^\circ$ ) the critical geometry of the city's slope. Figure 12 shows the variation of FS throughout the earthquake period.

The factor of safety swayed with the variation of acceleration along seismic waves initiating instability and risky state on the slope, where the FS reaches a value less than unity. Figure 13 compares the FSs before and after the earthquake. The FS decreased more than 81% from their original FS before the quake. The effect of earthquakes on slope stability can be understood as an equivalent increase in the inclination of joint failure plane [34]. The inspected slope within the study area failed after being exposed to the earthquake for the investigated parameters when it was not even severed from footing loads.

To express the huge damage that the existing constructions in the studied area could suffer, the seismic loading impact was examined with a combination of footing. Figure 14 compares the FSs before and after the seismic event for different footing width ( $B$ ). After the earthquake, the FSs dropped by 68-78%, with larger  $B$  indicating a higher percentage drop.

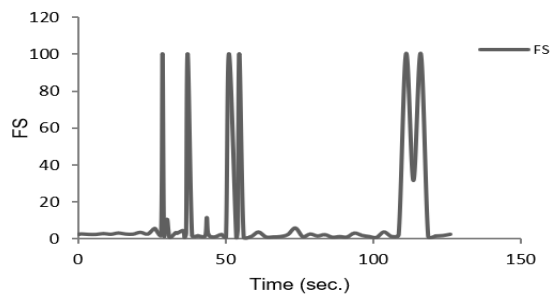


**Figure 12.** FS change along earthquake period for slope without footing, (H)=30m and ( $\theta$ )=15 deg

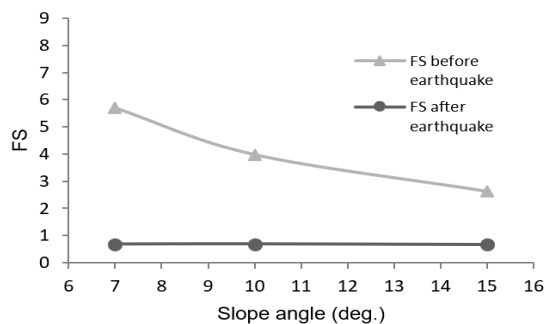


**Figure 13.** The effect of earthquake on factor of safety on slopes without footing (H=30m)

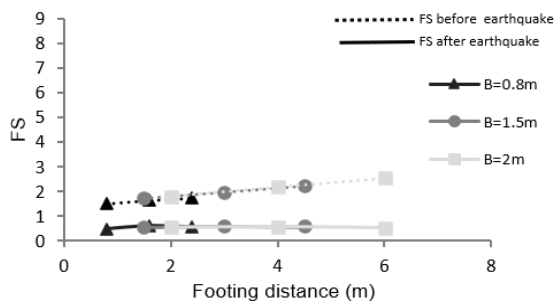


**Figure 14.** The effect of earthquake on factor of safety on slopes with footing B=(0.8, 1.5 and 2)m for slope (H=30m, $\theta$ =15°)

This reduction in FS is caused by the irritation effect of the dynamic load created on the superstructure generating extra forces which are transported to the footings, causing an additional decrease in the bearing capacity ( $q_u$ ). The results gave a minimum and maximum FS equal to 0.48 and 0.58 respectively.

#### 4. CONCLUSIONS

The recent paper investigates the effect of neighboring footing and seismic forces on the stability of Al-Najaf

city slopes numerically. The following conclusions can be drawn from the above research:

- The smallest value of the factor of safety is around 2.6, implying that the slope in Al-Najaf is safe in regards to the investigated slope characteristics without loading.
- The slopes' inclined angle ( $\theta$ ) had the greatest influence on safety (in reverse proportion), while the height had only a minor effect under the scenarios of slope geometry and no loading.
- The impact of footing on slope stability in the study area is local (due to bearing capacity failure) concerning the investigated footing width (B), distance (X), and stress (85kPa). As a maximum value, the FS is reduced to less than 1.8.
- The factor of safety increases with the increasing of the footing distance ratio (X/B) until distance beyond (X/B=4) where the increase reduces as the bearing capacity of the footing on slope approaches that of a footing on level ground.
- During the earthquake, the FS of the slope is less than unity with its own weight for all investigated slope geometry. The FSs values are reduced by approximately 81%.
- When neighbour footing and seismic loads are applied, the FS of slope was reduced by about 68-78% compared to the static footing state.
- The current structures built on the slope of Al-Najaf are vulnerable to collapse and destruction in the event of an earthquake similar to the one used in the investigation modelling.

#### 5. REFERENCES

1. Mahmood, M.S., Akhtarpoor, A. and Alsharifi, Z., "A review of slopes stability challenges and neighbour buildings", in *Journal of Physics: Conference Series*, IOP Publishing. Vol. 1895, No. 1, (2021), 012014.
2. Budhu, M., *Soil mechanics and foundation-3rd edition* john wiley & sons inc. 2010, ISBN 978-040-55684-9.
3. Cruden, D. and Varnes, D., *Landslide types and processes. Landslides: Investigation and mitigation (ed. Turner, ak and schuster, rl), special report 247 of the transport research board, national research council.* 1996, National Academy Press, Washington DC.
4. Samani, H.M. and Meidani, M., "Slope stability analysis using a non-linear optimization technique (research note)", *International Journal of Engineering*, Vol. 16, No. 2, (2003), 147-156, doi.
5. Mofidi Rouchi, J., Farzaneh, O. and Askari, F., "Bearing capacity of strip footings near slopes using lower bound limit analysis", *Civil Engineering Infrastructures Journal*, Vol. 47, No. 1, (2014), 89-109, <https://dx.doi.org/10.7508/cej.2014.01.007>.

6. Supandi, S., "Simple slope stabilization on quartz sandstone using horizontal drain", *International Journal of Engineering*, Vol. 34, No. 4, (2021), 1046-1051, doi.
7. Raj, D., Singh, Y. and Kaynia, A.M., "Behavior of slopes under multiple adjacent footings and buildings", *International Journal of Geomechanics*, Vol. 18, No. 7, (2018), 04018062, [https://doi.org/10.1061/\(ASCE\)GM.1943-5622.0001142](https://doi.org/10.1061/(ASCE)GM.1943-5622.0001142).
8. Nadi, B., Askari, F. and Farzaneh, O., "Seismic performance of slopes in pseudo-static designs with different safety factors", *Iranian Journal of Science Technology. Transactions of Civil Engineering*, Vol. 38, No. C2, (2014), 465, doi.
9. Al-Ameri, A., Jawad, F. and Fattah, M., "Vertical and lateral displacement response of foundation to earthquake loading", *International Journal of Engineering*, Vol. 33, No. 10, (2020), 1864-1871, doi.
10. Barmenkova, E., "Design of base and foundation for the earthquake-resistant building", in IOP Conference Series: Materials Science and Engineering, IOP Publishing. Vol. 661, No. 1, (2019), 012093. <https://doi.org/10.1088/1757-899X/661/1/012093>
11. Majdi, A., "Earthquake hazard mitigation in iraq: Recommendations to decision makers", (2020).
12. Loukidis, D., Bandini, P. and Salgado, R., "Stability of seismically loaded slopes using limit analysis", *Geotechnique*, Vol. 53, No. 5, (2003), 463-479.
13. Mahmood, M.S., "Effect of time-based soaking on shear strength parameters of sand soils", *Applied Research Journal*, Vol. 3, No. 5, (2017), 142-149.
14. Mahmood, M.S., Al-Baghdadi, W.H., Rabee, A.M. and Almahbobi, S.H., "Reliability of shear-box tests upon soaking process on the sand soil in al-najaf city", in Key Engineering Materials, Trans Tech Publ. Vol. 857, (2020), 212-220. <https://doi.org/10.4028/www.scientific.net/kem.857.212>
15. Mahmood, M.S., Akhtarpour, A., Almahmodi, R. and Husain, M.M.A., "Settlement assessment of gypseous sand after time-based soaking", in IOP Conference Series: Materials Science and Engineering, IOP Publishing. Vol. 737, No. 1, (2020), 012080. <https://doi.org/10.1088/1757-899X/737/1/012080>
16. Mahmood, M.S. and Abraham, M.J., "A review of collapsible soils behavior and prediction", in IOP Conference Series: Materials Science and Engineering, IOP Publishing. Vol. 1094, No. 1, (2021), 012044. DOI: 10.1088/1757-899X/1094/1/012044
17. Sh, M.M., Akhtapour, A. and AA, A.A., "Mechanical behavior of dam-vertically sand drained foundation, case study: Sombar dam", *Journal of Engineering and Technological Sciences*, Vol. 51, No. 3, (2019), DOI: 10.5614/j.eng.technol.sci.2019.51.3.6
18. Akhtarpour, A., Mahmood, M.S. and Alali, A., "Evaluation of vertical drain with different materials", in IOP Conference Series: Materials Science and Engineering, IOP Publishing. Vol. 584, No. 1, (2019), 012011. DOI:10.1088/1757-899X/584/1/012011
19. Akhtarpour, A., Mahmood, M.S. and Alali, A., "Stability analysis of geosynthetically piled foundation earth dam; a case study: Sombar dam", in IOP Conference Series: Materials Science and Engineering, IOP Publishing. Vol. 888, No. 1, (2020), 012003. DOI:10.1088/1757-899X/888/1/012003
20. Liu, S., Shao, L. and Li, H., "Slope stability analysis using the limit equilibrium method and two finite element methods", *Computers Geotechnics*, Vol. 63, (2015), 291-298, doi.
21. Duncan, J.M., "State of the art: Limit equilibrium and finite-element analysis of slopes", *Journal of Geotechnical Engineering*, Vol. 122, No. 7, (1996), 577-596, <https://doi.org/10.1016/j.compgeo.2014.10.008>
22. Al-Taie, A.J. and Albusoda, B.S., "Earthquake hazard on iraqi soil: Halabjah earthquake as a case study", *Geodesy Geodynamics*, Vol. 10, No. 3, (2019), 196-204, <https://doi.org/10.1016/j.geog.2019.03.004>.
23. Al-Saoudi, N.K. and Al-Shakerchy, M.S.M., "Statistical analysis of some geotechnical properties of najaf city", in Proceedings of International Geotechnical Conference. Vol. 3, (2010), 1173-1180.
24. Alzabeebee, S. and Ammash, H., "Effect of presence of cavity on behavior of strip foundation rested on al-najaf soil as case study", in the Proceeding of the 2nd international conference on engineering, university of Mosul, Iraq. (2013), 1-11.
25. Devi, D.D.L. and Anbalagan, R., "Study on slope stability of earthen dams by using geostudio software", *International Journal of Advanced Research, Ideas Innovations in Technology*, Vol. 3, No. 6, (2017), 408-414.
26. Das, B.M., "Principles of geotechnical engineering, Cengage learning, (2021).
27. Ti, K.S., Huat, B.B., Noorzaei, J., Jaafar, M.S. and Sew, G.S., "A review of basic soil constitutive models for geotechnical application", *Electronic Journal of Geotechnical Engineering*, Vol. 14, (2009), 1-18.
28. Krahn, J., "Dynamic modeling with quake/w: An engineering methodology, GEO-SLOPE Calgary, (2004).
29. Seed, H.B., Idriss, I.M., Lee, K.L. and Makdisi, F.I., "Dynamic analysis of the slide in the lower san fernando dam during the earthquake of february 9, 1971", *Journal of the Geotechnical Engineering division*, Vol. 101, No. 9, (1975), 889-911.
30. Kramer, S.L., "Geotechnical earthquake engineering, Pearson Education India, (1996).
31. Sazzad, M. and Haque, M., "Effect of surcharge on the stability of slope in a homogeneous soil by fem", in 2nd International Conference on Advances in Civil Engineering. (2014), 315-318.
32. Plummer, C.C., Carlson, D.H. and Hammersley, L., "Physical geology, New York, NY: McGraw-Hill/Education, Inc., (2016).
33. Keskin, M.S. and Laman, M., "Model studies of bearing capacity of strip footing on sand slope", *Journal of Civil Engineering*, Vol. 17, No. 4, (2013), 699-711, <https://doi.org/10.1007/s12205-013-0406-x>.
34. Ling, H.I. and Cheng, A.H.-D., "Rock sliding induced by seismic force", *International Journal of Rock Mechanics Mining Sciences*, Vol. 34, No. 6, (1997), 1021-1029, DOI: 10.1016/S0148-9062(97)00261-1.



---

**Persian Abstract**

---

**چکیده**

انتظار می رود در سالهای آینده النجف ، یکی از مهمترین شهرهای عراق رشد کند. بسیاری از ساختمانهای واقع در دامنه های النجف ، که نزدیک حرم امام علی است ، دارای ارزشهای اقتصادی و گردشگری مهمی هستند. در این مقاله ثبات شیب شهر تحت شرایط مختلفی از جمله هندسه شیب ، بارگذاری ساختار همسایه و بزرگی زمین لرزه بررسی می شود. در تجزیه و تحلیل یک روش اجزای محدود  $D\alpha$  با کمک رایانه استفاده شده است. مجموعه ای از آزمایش های طبقه بندی و شناسایی خاک علاوه بر پارامترهای مورد نیاز خاک در مدل سازی سازه انجام می شود. مدل Mohr-Coulomb برای تعریف وضعیت خرابی که از شیب آغاز شده استفاده می شود. نتایج نشان می دهد که شیب به دلیل وزن و هندسه پایدار است و حداقل ضریب ایمنی آن ۲.۶ است. در حالی که تحت بارگذاری قرار می گیرید ، این ضریب ایمنی به کمتر از ۱.۸ کاهش می یابد. خطرناکترین شرایط زمانی است که دامنه تحت بارگذاری لرزه ای قرار گرفته باشد و ضریب ایمنی کمتر از یک واحد باشد ، برای همه موارد و خصوصیات بررسی شده ، جایی که دامنه ها فرو می ریزند.

---